Highly efficient reduced graphene oxide mode-locked Nd:GGG laser

Chunhua Zuo (左春华)[1], Jia Hou (侯 佳)[2], Baitao Zhang (张百涛)[2,*], and Jingliang He (何京良)[2]

[1]*School of Mathematics, Qilu University of Technology, Jinan 250100, China*
[2]*State Key Laboratory of Crystal Materials, Shandong University, Jinan 250100, China*
**Corresponding author: bai3697@126.com*

Received September 29, 2014; accepted November 14, 2014; posted online February 9, 2015

We report, for the first time to our knowledge, a diode-end-pumped passively mode-locked (ML) Nd-doped gadolinium gallium garnet laser based on a chemically reduced graphene oxide (RGO) saturable absorber mirror. The ML laser gives a pulse duration of 15.1 ps under the maximum average output power of 1.44 W, corresponding to a slope efficiency of 21.1%. The single-pulse energy and peak power are 21.6 nJ and 1.43 kW, respectively. The results indicate that our RGO saturable absorber has promising prospects for applications in high-power and high-efficiency ultrafast lasers.

OCIS codes: 140.3460, 140.3538, 140.4050.
doi: 10.3788/COL201513.021401.

Ultra-short pulse lasers have been widely used in the fields of metrology, ultrafast spectroscopy, ultrafast capacity optical communication, superfine materials processing, microscopy, and so on. In the past 2 decades, semiconductor (SE) saturable absorber mirrors (SAMs) have been widely employed as intra-cavity optical modulators for ultra-short pulse generation[1–3]. There is no denying that SESAM has made great contributions to improving the performance of solid-state mode-locked (ML) lasers. However, their applications have been limited due to the relatively narrow operating wavelength range. Single-walled carbon nanotubes (SWCNTs), as another alternative, can realize a wide saturable absorption band by mixing SWCNTs of different tube diameters. However, a large insertion loss is introduced[4–6]. Recently, graphene has proven to be a future material with plenty of useful characters. In laser devices, it is an ideal saturable absorber due to a number of remarkable properties, such as fast recovery time, amazing thermal conductivity, strong saturable absorption, large modulation depth, low optical loss, and easy mass-fabrication[7–11]. In a respect that is superior to traditional saturable absorbers, graphene theoretically can be adapted to any wavelength excitation because of the gapless linear dispersion of Dirac electrons. Much effort has been done to develop graphene saturable absorber-based lasers in the 1.0, 1.3, 1.5, and 2 μm regions[7–16], and it has shown good performance in both *Q*-switched and ML operation. Furthermore, graphene oxide (GO) and reduced graphene oxide (RGO) are outstanding in terms of fabrication, the procedures for which are low-cost and highly productive. It has been experimentally demonstrated that RGO has high potential for development of a high-power ultrafast laser. Layered GO was first dispersed in water by using a modified Hummers' method. Then layered RGO was obtained by reducing the GO layers in hydrazine at 95°C for 2 h. For the last step, the RGO solution was sonicated and spin-coated on the BK7 glass substrate and then dried in a vacuum oven at 80°C for 24 h. Defects could be observed in the Raman spectrum as there was a high D peak, and the layer number was determined to be 1 to 5 by using atomic force microscopy (AFM) and high-resolution transmission electron microscopy (HRTEM)[13].

As a host material, gadolinium gallium garnet ($Gd_3Ga_5O_{12}$, i.e., GGG) possesses many excellent properties including easy growth and no core, high thermal conductivity, good mechanical properties, large thermal capacity, wider phase homogeneity with a high pulling rate (up to 5 mm/h), and so on[17–19]. Nd^{3+} ion doped GGG crystals (Nd:GGG) have attracted much attention and have been widely studied and applied in recent years[19–23]. In previous works, it has been shown that this crystal could have highly efficient continuous-wave (CW) and passive *Q*-switched operations. A ML Nd:GGG laser can be easily obtained theoretically owing to the large stimulated emission cross section of $2.1 \pm 0.1 \times 10^{-19}$ cm^2[24]. A SESAM ML Nd:GGG laser with an average output power of 0.4 W and a pulse duration of 17.5 ps was reported[20]. However, there are no reports about a graphene ML Nd:GGG laser, and it promoted us to research its performance in high-power ML lasers based on RGO saturable absorbers.

In this Letter, we are the first, to the best of our knowledge, to report a diode-end-pumped, high-power, and high-efficiency CWML Nd:GGG laser based on RGO. A stable ML pulse with a pulse duration of 15.1 ps was obtained with a pulse repetition rate of 66.8 MHz, and the maximum average output power was as high as 1.44 W.

The experimental setup is schematically shown in Fig. 1. The pump source is an 808 nm fiber-coupled diode laser capable of delivering a maximum output power of 30 W.

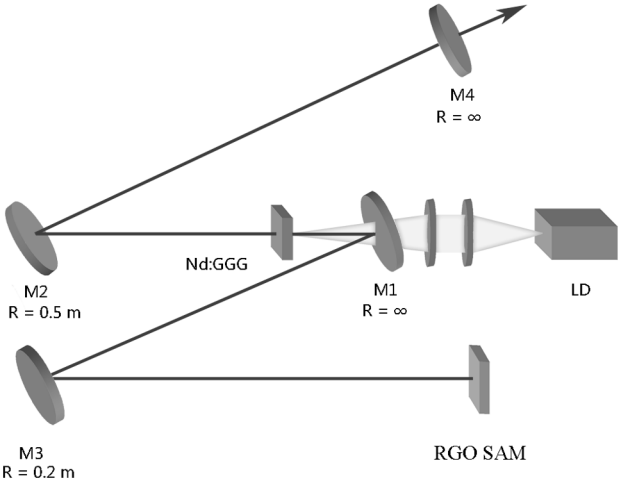

Fig. 1. Configuration of the RGO MLNd:GGG laser.

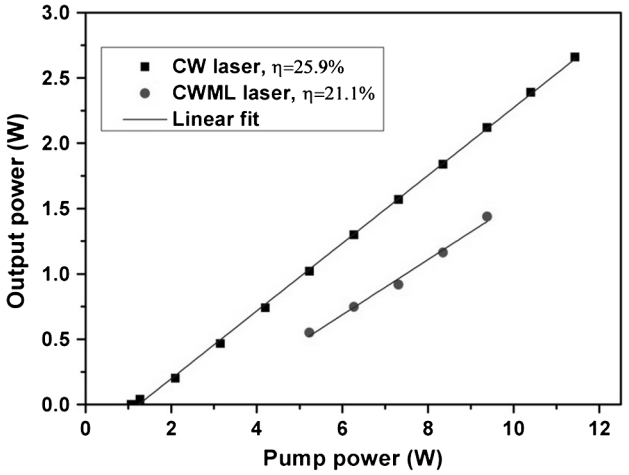

Fig. 2. CW and ML output power versus absorbed pump power.

The fiber has a core diameter of 400 μm and a numerical aperture of 0.22. Its radiation is coupled into the laser crystal by a focusing optical system. The beam spot radius generated in the crystal was 200 μm. A Nd:GGG crystal with dimensions of 4 mm × 4 mm × 5 mm is used for the laser operation, and it is antireflection (AR)-coated for 808 and 1062 nm on both end faces. The laser crystal is wrapped with indium foil and mounted in the copper block cooled by water at a temperature of 15°C. The RGO SAM used in this work is the same SAM that we fabricated and used[13]. It should be mentioned that the modulation depth was about 13%. In order to obtain stable and efficient mode-locking, we used a W-shaped laser cavity with two collimated arms to ensure a proper beam size in the crystal and on the graphene RGO SAM. Mirror 1 is a flat mirror that is AR-coated at 808 nm ($R < 0.2\%$) on the outside surface, high-reflectance (HR) coated at 1062 nm ($R > 99.8\%$) and high-transmission (HT) coated at 808 nm on the inside surface. Mirrors 2 and 3 are folded mirrors with the radii of curvature of 500 and 200 mm, respectively, and are HR-coated at 1062 nm. The RGO SAM is employed both as a saturable absorption element and HR-end mirror. Mirror 4 is the output coupler with a transmittance of 10%. The laser mode radii in the crystal and graphene RGO SAM were calculated to be ∼210 and ∼50 μm. The laser pulse signal was recorded by a Tektronix DPO7104 digital oscilloscope (1 GHz bandwidth, 5 Gs/s sampling rate) and a photo-detector (New Focus, Model 1611). The average output power was measured by a laser power meter (Field-Max II, Coherent). The pulse duration of the ML laser was measured by a commercial autocorrelator (APE, Pule Check 150).

Figure 2 shows the dependence of output power on the pump power for the CW and ML operation.

Like other diode-end-pumped ML lasers, the ML Nd:GGG laser showed two regimes of ML operation. With careful adjustment of the cavity elements, a metastable Q-switched mode-locked (QML) regime was observed as soon as the absorbed pump power reached the threshold condition of 1.2 W. When the absorbed pump power was beyond 5.2 W, the QML operation was overcome and a steady-state CWML state was obtained. A typical CWML pulse train in different time scales is shown in Fig. 3.

The pulse repetition rate was 66.8 MHz, which corresponds to a cavity length of 2.24 m. The single-pulse energy was calculated to be 21.6 nJ, and the pulse-to-pulse intensity fluctuation is estimated to be less than 3%. A radio frequency spectrum analyzer was used to further clarify the pulse stability, and the recorded result is shown in Fig. 4.

A maximum average CWML output power of 1.44 W was obtained under the absorbed pump power of 9.38 W, corresponding to an optical-to-optical conversion efficiency of 15.4% and a slope efficiency of 21.1%. If pump power was below 5.23 W or above 9.38 W, the laser was in a QML regime due to improper fluence on the RGO SAM. The output power is much higher than that obtained by the SESAM ML Nd:GGG laser reported[20] (400 mW). It is attributed to several reasons: higher transmittance of the output coupler, larger mode radii in the crystal and on the RGO SAM (which will lead to better

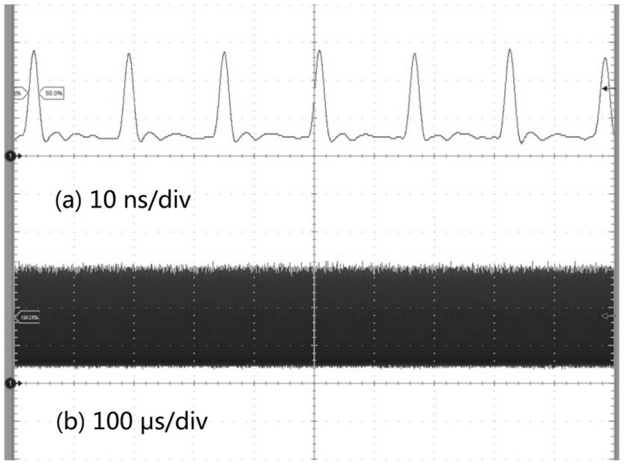

Fig. 3. Oscilloscope traces of the CWML pulse trains.

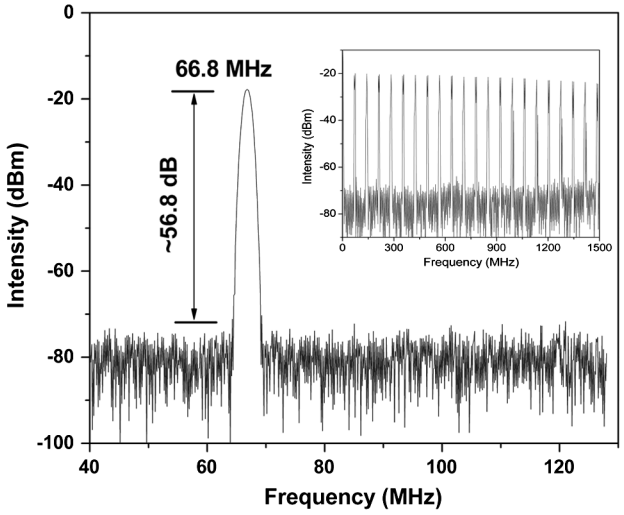

Fig. 4. RF spectrum of Nd:GGG RGO ML laser.

energy extraction and high threshold of mode-locking), and lower nonsaturable loss of the RGO SAM compared with SESAM. The ML pulses exhibited good stability in either the nanosecond or microsecond timescale. The mode-locking could self-start and remain sustained when the absorbed pump power was recovered above the threshold again. We replaced the RGO SAM with a plane mirror to make sure that the mode-locking operation was produced by the RGO SAM. Throughout the test, only stable CW laser operation was obtained and no pulsed regime was observed. The maximum CW output power was 2.66 W under a pump power of 11.43 W. From Fig. 2, one can get that the relationship of the output power between the graphene mode-locking and the CW operations. The ratio reaches a high value of 67.9% (with a CW output power of 2.12 W and mode-locking output power of 1.44 W under a pump power of 9.4 W), indicating a large insertion loss of the RGO sheets; the performance can be improved along with upgrading of the preparation process of large-area monolayer RGO layers. Figure 5 shows the measured spatial beam profile under the maximum ML output power; the quality parameter M2 factor was 1.64 and 1.53 in the horizontal and longitudinal planes, respectively.

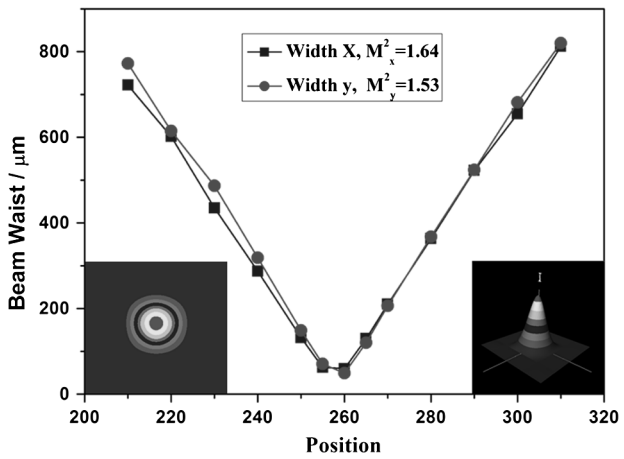

Fig. 5. Measured beam quality parameter M^2 factor and spatial beam profile under the maximum ML output power.

The spectrum of the ML laser is shown in Fig. 6(a). It has a FWHM of about 0.145 nm. The measured autocorrelation is shown in Fig. 6(b). The FWHM of the autocorrelation trace is about 21.3 ps. Then the pulse duration of the ML pulse is about 15.1 ps, assuming a Gaussian pulse shape. The pulse duration is shorter than the ML SESAM reported previously[20] (17.3 ps). Therefore, the time-bandwidth product of the pulses is calculated to be 0.462, which is 1.05 times the value of a transform-limited Gaussian pulse. The results manifest the advantages of RGO as mode-lockers when compared with other saturable absorbers.

In conclusion, we obtain highly efficient diode-end-pumped ML Nd:GGG lasers based on a RGO SAM; the highest average output power is 1.44 W with a slope efficiency of 21.1%. The ML pulse duration is estimated to be 15.1 ps with a pulse repetition rate of 66.8 MHz. The single-pulse energy and peak power are determined to be 21.6 nJ and 1.43 kW, respectively. Compared with other SESAM ML Nd:GGG lasers previously reported,

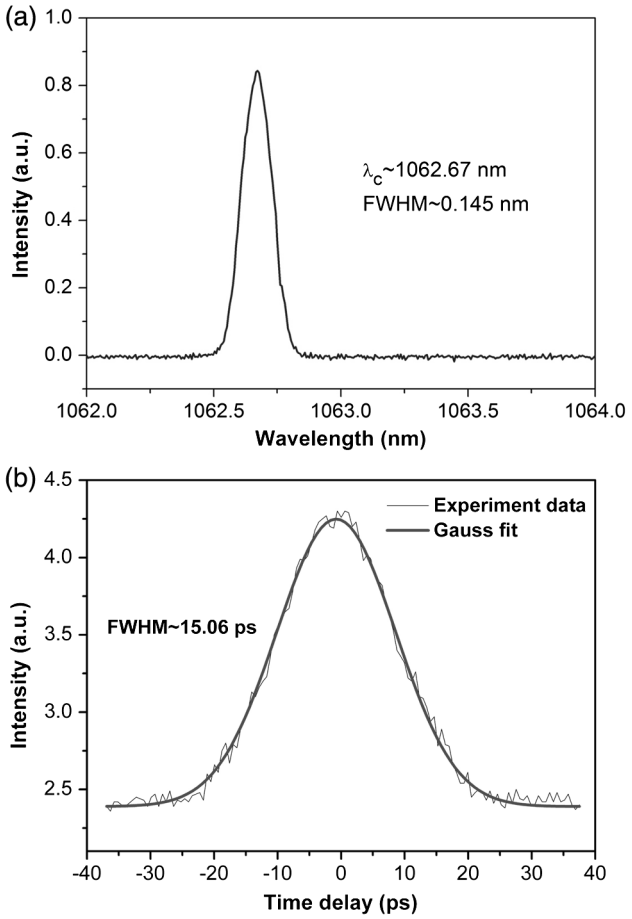

Fig. 6. (a) Measured spectrum of the ML pulses; (b) autocorrelation trace of the ML pulses. Assuming a Gaussian pulse shape, the pulse duration is about 15.1 ps.

our results indicate that RGO is suitable for obtaining high-power and high-efficiency ultrafast lasers.

This work was supported by the National Natural Science Foundation of China (Nos. 61308042 and 51321091), the Project of Shandong Province Higher Educational Science and Technology Program (No. J11L13), and the Key Laboratory of Functional Crystal Materials and Device (Shandong University), Ministry of Education (No. KF1207).

References

1. U. Keller, K. J. Weingarten, F. X. Kärtner, D. Kopf, B. Braun, I. D. Jung, R. Fluck, C. Hönninger, N. Matuschek, and J. Aus der Au, IEEE J. Sel. Top. Quantum Electron. **2**, 435 (1996).
2. X. Yin, J. Meng, J. Zu, and W. Chen, Chin. Opt. Lett. **11**, 081402 (2013).
3. X. Fu, J. Li, and X. Liang, Chin. Opt. Lett. **11**, 081401 (2013).
4. Y.-C. Chen, N. R. Raravikar, L. S. Schadler, P. M. Ajayan, Y.-P. Zhao, T.-M. Lu, G.-C. Wang, and X.-C. Zhang, Appl. Phys. Lett. **81**, 975 (2002).
5. T. R. Schibli, K. Minoshima, H. Kataura, E. Itoga, N. Minami, S. Kazaoui, K. Miyashita, M. Tokumoto, and Y. Sakakibara, Opt. Express **13**, 8025 (2005).
6. W. B. Cho, J. H. Yim, S. Y. Choi, S. Lee, U. Griebner, V. Petrov, and F. Rotermund, Opt. Lett. **33**, 2449 (2008).
7. T. Hasan, Z. Sun, F. Wang, F. Bonaccorso, P. H. Tan, A. G. Rozhin, and A. C. Ferrari, Adv. Mater. **21**, 3874 (2009).
8. Q. L. Bao, H. Zhang, Y. Wang, Z. H. Ni, Y. L. Yan, Z. X. Shen, K. P. Loh, and D. Y. Tang, Adv. Funct. Mater. **19**, 3077 (2009).
9. H. Zhang, D. Y. Tang, R. K. Knize, L. M. Zhao, Q. L. Bao, and K. P. Loh, Appl. Phys. Lett. **96**, 111112 (2010).
10. A. Martinez, K. Fuse, and S. Yamashita, Appl. Phys. Lett. **99**, 121107 (2011).
11. D. Popa, Z. Sun, F. Torrisi, T. Hasan, F. Wang, and A. C. Ferrari, Appl. Phys. Lett. **97**, 203106 (2010).
12. Z. Sun, D. Popa, T. Hasan, F. Torrisi, F. Wang, E. Kelleher, J. Travers, V. Nicolosi, and A. Ferrari, Nano Res. **3**, 653 (2010).
13. F. Lou, L. Cui, Y. Li, J. Hou, J. He, Z. Jia, J. Liu, B. Zhang, K. Yang, Z. Wang, and X. Tao, Opt. Lett. **38**, 4189 (2013).
14. J. L. Xu, X. L. Li, Y. Z. Wu, X. P. Hao, J. L. He, and K. J. Yang, Opt. Lett. **36**, 1948 (2011).
15. J. L. Xu, X. L. Li, J. L. He, X. P. Hao, Y. Yang, Y. Z. Wu, S. D. Liu, and B. T. Zhang, Opt. Lett. **37**, 2652 (2012).
16. J. Ma, G. Q. Xie, W. L. Gao, P. Yuan, L. J. Qian, H. H. Yu, H. J. Zhang, and J. Y. Wang, Opt. Lett. **37**, 2085 (2012).
17. H. Hayakawa, K. Maeda, T. Ishikawa, T. Yokoyama, and Y. Fuji, Jpn. J. Appl. Phys. **26**, L1623 (1987).
18. B. Labranche, Q. Wu, and P. Galarneau, Proc. SPIE **2041**, 326 (1998).
19. Z. T. Jia, X. T. Tao, C. M. Dong, J. Zhang, H. J. Zhang, Z. P. Wang, and M. H. Jiang, J. Cryst Growth **292**, 386 (2006).
20. L. J. Qin, D. Y. Tang, G. Q. Xie, H. Luo, C. M. Dong, Z. T. Jia, H. H. Yu, and X. T. Tao, Opt. Commun. **281**, 4762 (2008).
21. C. H. Zuo, J. L. He, H. T. Huang, B. T. Zhang, Z. T. Jia, C. M. Dong, and X. T. Tao, Opt. Laser Technol. **41**, 17 (2009).
22. C. H. Zuo, B. T. Zhang, J. L. He, X. L. Dong, J. F. Yang, H. T. Huang, J. L. Xu, S. Zhao, C. M. Dong, and X. T. Tao, Appl. Phys. B **95**, 75 (2009).
23. H. T. Huang, J. L. He, B. T. Zhang, J. F. Yang, J. L. Xu, C. H. Zuo, and X. T. Tao, Opt. Express **18**, 3352 (2010).
24. M. D. Rotter and B. Dane, Opt. Commun. **198**, 155 (2001).